

Review Commentary

Photoinduced electron transfer and strand cleavage in pyrenyl–DNA complexes and adducts

Nicholas E. Geacintov,* Kyril Solntsev, Lawrence W. Johnson, Junxin Chen, Alexander D. Kolbanovskiy, Tongming Liu and Vladimir Ya. Shafirovich

Chemistry Department, New York University, New York, NY 10003-5180, USA

Received 22 September 1997; revised 20 February 1998; accepted 25 February 1998

ABSTRACT: The fluorescence of pyrenyl residues in complexes with the nucleic acid bases G, C and T, but not A, is strongly quenched by photoinduced electron transfer mechanisms. Site-specifically modified 11-mer oligonucleotide duplexes containing a single modified guanosyl base G* bearing a covalently attached pyrenyl residue were prepared in order to probe for photochemical damage associated with these photoinduced electron transfer reactions. When the pyrenyl residue positioned at G* is photoexcited with 355 nm light, direct strand cleavage is observed at that site with low quantum yield. Frank strand breaks are also observed up to five base pairs away from G*, suggesting that intrastrand migration of a reactive intermediate from base to base is occurring. © 1998 John Wiley & Sons, Ltd.

KEYWORDS: pyrenyl–DNA complexes and adducts; photoinduced electron transfer; strand cleavage

INTRODUCTION

Electron transfer reactions in DNA are a subject of great current interest (see, for example, Refs 1–3). Upon photoexcitation of a fluorophore or photosensitizer molecule bound to DNA, electron transfer reactions with one of the adjacent DNA bases may occur if the redox potentials of the donor–acceptor couple are favorable. The intermediate radical ion pairs thus generated can either recombine, thus regenerating the singlet excited state of the fluorophore, or decay radiatively via an exciplex state^{4,5} or non-radiatively to the triplet excited state or ground state^{6,7} of the fluorophore or photosensitizer molecules. Alternatively, the primary radical ion pair can initiate a series of chemical reactions which culminate in DNA strand cleavage or other forms of DNA damage.^{2,3,8–10} The detailed characterization of these processes is important for gaining a better understanding of the mechanisms by which nucleic acids quench the fluorescence of photosensitizers, and the reaction pathways that lead to DNA damage by type I electron transfer mechanisms.¹⁰ In this paper, we briefly describe some of our recent work in this area of research using pyrene derivatives bound covalently and non-

covalently to nucleic acids (see, for example, Refs 5–8 and 11–13).

THE PYRENYL MODEL SYSTEM

Benzo[*a*]pyrene (B[*a*]P), a ubiquitous environmental pollutant, is metabolized in living cells to a variety of oxygenated derivatives, including the bay region diol epoxides *r*7,*t*8-dihydroxy-*t*9,10-epoxy-7,8,9,10-tetrahydroB[*a*]P (*anti*-BPDE, or simply BPDE, Fig. 1). The (+)-7*R*,8*S*,9*S*,10*R* and (–)-7*S*,8*R*,9*R*,10*S* enantiomers of BPDE react with the exocyclic amino groups of 2'-deoxyadenosine (dA) or 2'-deoxyguanosine (dG) residues in native DNA to form covalent adducts. The reactions can occur either by *trans* or by *cis* addition of dG or dA relative to the epoxide moiety at the C-10 position of BPDE (Fig. 1). BPDE can also react with water to form the non-toxic and non-reactive tetraol 7,8,9,10-tetrahydroxy-tetrahydrobenzo[*a*]pyrene (BPT, Fig. 1). The photoactive chromophore is the pyrenyl residue (Py) in all cases.

PHOTOINDUCED ELECTRON TRANSFER AND QUENCHING OF THE FLUORESCENCE OF PY RESIDUES

The fluorescence decay characteristics of BPT and various covalent adducts derived from the binding of BPDE to dG or dA are summarized in Table 1. The

*Correspondence to: N. E. Geacintov, Chemistry Department, New York University, New York, NY 10003-5180, USA.

Contract/grant sponsor: National Science Foundation; contract grant number: CHE-9700429.

Contract/grant sponsor: National Institutes of Health; contract grant number: 1 F33 GM17908.

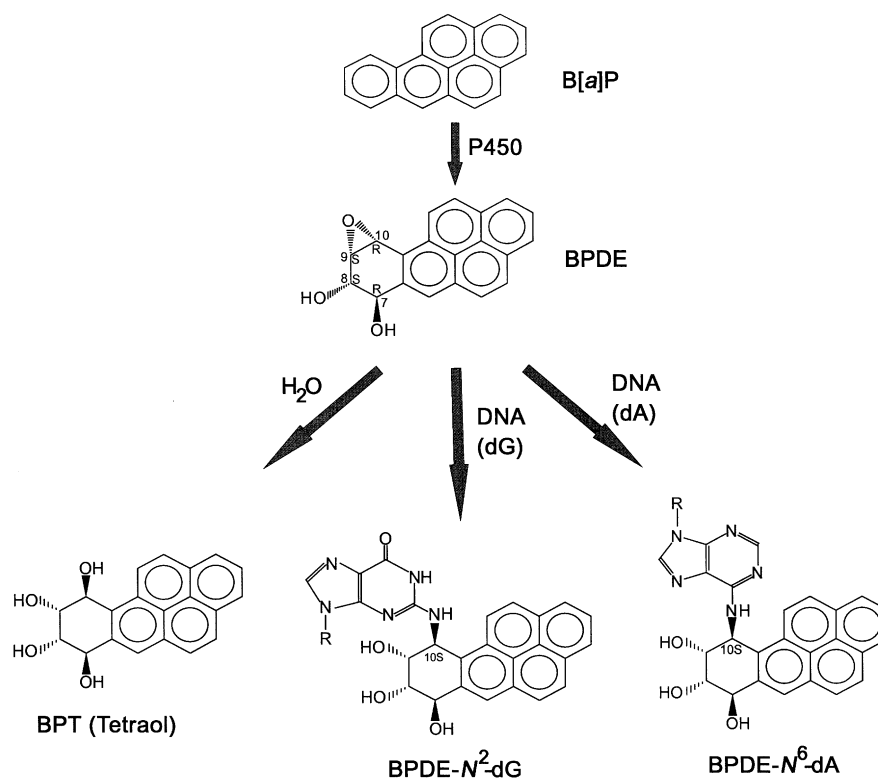


Figure 1. Metabolism of B[a]P to diol epoxides BPDE [the (+)-7R,8S,9S,10R enantiomer is shown] and reactions of BPDE with water to form the tetraols BPT, with DNA to form the covalent adducts shown [the 10S(+)-*trans*-adducts are depicted in each case].

Table 1. Fluorescence lifetimes of selected adducts derived from the binding of BPDE to dA, dG or oligonucleotides^a

Substance	τ_1 (ns) (A_1)	τ_2 (ns) (A_2)	τ_3 (ns) (A_3)	τ_{mean} (ns)
BPT	200 ± 5 (1.0)	—	—	200 ± 5
(+)- <i>trans</i> -BPDE-N ² -dG	1.4 ± 0.1 (1.0)	—	—	1.4 ± 0.1
(+)- <i>cis</i> -BPDE-N ² -dG	0.41 (0.83)	2.2 (0.17)	—	0.71 ± 0.2
(+)- <i>cis</i> -BPDE-N ⁶ -dA (A_3)	180 ± 5 (1.0)	—	—	180 ± 5
5'-dCpA*	20.8 (0.72)	4.9 (0.28)	—	16.4 ± 2
5'-dA*pC	76.2 (0.99)	20.4 (0.01)	—	74.9 ± 3
5'-dCpA*pC	28.1 (0.54)	7.6 (0.46)	—	18.7 ± 1
5'-d(CTCTCA*CTTCC)	0.70 (0.53)	3.7 (0.36)	12.9 (0.11)	3.1 ± 0.4
5'-d(CTCTCA*CTTCC) · 3'-d(GAGAGTGAAGG)	0.60 (0.67)	3.4 (0.25)	13.8 (0.08)	2.3 ± 0.3

^a The τ_i and A_i terms are defined in Eqn (1).

fluorescence lifetime, τ , of BPT in oxygen-free aqueous buffer solutions (20 mM sodium phosphate buffer, pH 7.0) is 200 ± 5 ns. However, in complexes with native DNA, the fluorescence of BPT is strongly quenched.¹⁴ In aqueous solutions, BPT forms non-covalent ground-state association complexes with the 2'-deoxynucleosides dG, dA, dC and dT with association constants in the range ~10 to 200 l mol⁻¹.^{11,13}

All of these nucleosides, except dA, are strong quenchers of the fluorescence of BPT by a proton-coupled electron transfer mechanism¹³ involving both static (ground-state complex formation) and dynamic

quenching effects. The fluorescence lifetimes of the noncovalent BPT-dG, -dC and -dT complexes, inferred from the data in Ref. 13, are 5.3 ± 1.1, 5.6 ± 1.1 and 0.59 ± 0.12 ns, respectively; the fluorescence lifetimes of BPT in these association complexes is thus *ca* 30–300 times smaller than the lifetime of free BPT.

An analysis of the transient absorption spectra suggests that the Py residue is the electron acceptor in quenching interactions with guanine residues, and the electron donor in quenching interactions with dC and dT.^{12,13}

In covalent adducts, the fluorescence intensity decay profiles, $I(t)$, can be described in terms of 1–3 exponential

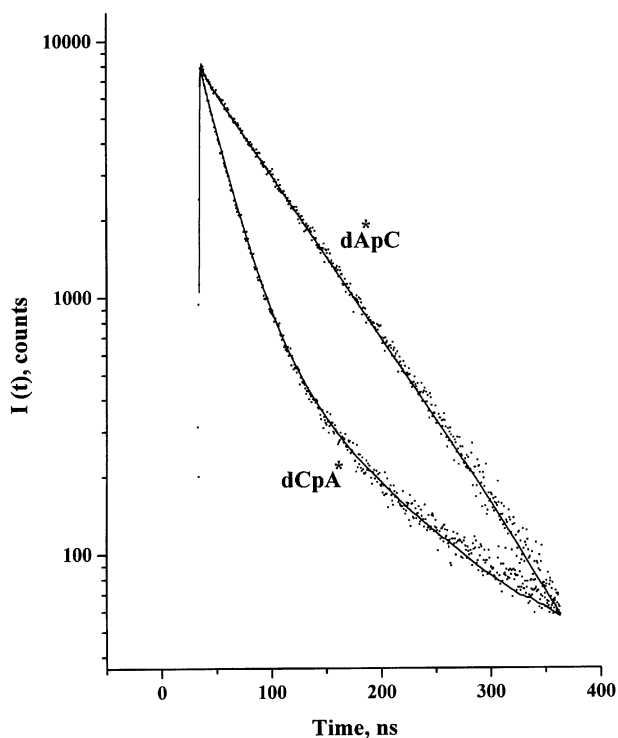


Figure 2. Fluorescence intensity decay profiles of dCpA* and dA*pC dinucleoside adducts with A* = (+)-*cis*-BPDE-*N*⁶-dA. Solid line, fits of Eqn (1) to the data points. The τ_i (A_i) values are shown in Table 1) with χ^2 values of 1.16 (dCpA*) and 1.04 (dA*pC).

components with lifetimes τ_i and amplitudes A_i ($\sum A_i = 1.0$):

$$I(t) = \sum_i A_i \exp(-t/\tau_i) \quad (1)$$

The fluorescence quantum yields of a particular adduct, Φ , relative to the yield of BPT is $\Phi = \tau_{\text{mean}}/\tau_{\text{BPT}}$ ($\tau_{\text{BPT}} = 200$ ns), and the mean fluorescence decay time is defined by $\tau_{\text{mean}} = \sum A_i \tau_i$.

In the covalent (+)-*trans*-BPDE-*N*²-dG mononucleoside adducts (Fig. 1) in aqueous solutions, the decay profiles are nearly monoexponential with decay times of 1.4 ± 0.1 ns (Table 1), implying that Φ is *ca* 130 times smaller than in the case of BPT. The quenching effect is strongly dependent on the stereochemical properties of the modified nucleosides since τ_{mean} of the (+)-*cis*-BPDE-*N*²-dG adduct is only *ca* 0.7 ns, and Φ is almost 300 times smaller than that of BPT. In contrast, in (+)-*trans*-BPDE-*N*⁶-dA mononucleoside adducts, the fluorescence yield of Py is not affected significantly (Table 1), regardless of the stereochemical adduct characteristics (data not shown). The relative efficiencies of quenching of the fluorescence of the Py residues by dA, dG, dC and dT, and also the direction of electron transfer, can be rationalized in terms of the redox potentials of the donor/acceptor pairs^{15,16} and the Rehm–Weller equation.¹⁷

The fluorescence of the Py residues in covalent BPDE-

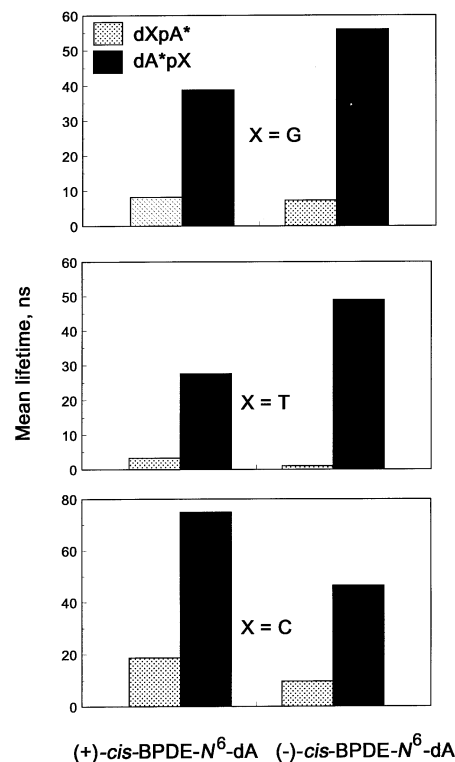


Figure 3. Mean fluorescence lifetimes of the Py residues in the sequence isomers dXpA* and dA*pX, with A* representing either the A* = (+)-*cis*- or (–)-*cis*-BPDE-*N*⁶-dA adducts.

*N*⁶-dA mononucleoside adducts is not quenched significantly. However, the fluorescence lifetimes are significantly diminished whenever the nucleotides dX = dG, dT or dC are attached to either the 5'- or the 3'-side of the BPDE-*N*⁶-dA moiety (Table 1). However, the fluorescence lifetimes are much shorter when dX is positioned on the 5'-side rather than the 3'-side of the modified adenine residue; this effect is illustrated in Fig. 2 which depicts the fluorescence intensity decay curves, $I(t)$, of a dXpA* and a dA*pX dinucleoside with A* = (+)-*cis*-BPDE-*N*⁶-dA (10*S* absolute configuration). As summarized in Fig. 3 the mean fluorescence lifetimes are significantly shorter when dX is positioned on the 5'-side (dXpA*) than on the 3'-side of A* (dA*pX). The dT residues are much stronger quenchers of the fluorescence of the Py residues in the dTpA* dinucleoside adducts than dC or dG in the dCpA* and dGpA* dinucleoside adducts. Similar sequence isomer effects are observed in the stereoisomeric (10*S*)-(+)-*trans*-, and (10*R*)-(–)-*trans*-dXpA* and dA*pX adducts (data not shown). The quenching efficiency is therefore not as strongly dependent on the orientations of the adenine residues relative to the *R* or *S* C-10 BPDE linkage site in A* as it is on the sequence. These results indicate that, on average, the Py and quencher base dX are closer to one another in the dXpA* than in the dA*pX adducts. Because of the

many variable torsion angles in these dinucleoside adducts, it is not possible to ascertain what these conformations might be without further experimental data or computations of the most probable conformations.¹⁸

When the BPDE-modified adenine residues A* are flanked by cytidine residues on both sides, the fluorescence of Py is strongly quenched since $\tau_{\text{mean}} = 18.7 \pm 1.0$ ns (Table 1). Similar quenching effects are observed when A* is flanked by dG or dT residues on both sides (data not shown). Interestingly, in the 11-mer oligonucleotide d(CTCTCA*CTTCC) with the modified adenine residue A* = (+)-*cis*-BPDE-*N*⁶-dA positioned in the center of the sequence, $\tau_{\text{mean}} = 3.1 \pm 0.4$ ns, which is significantly shorter than the 18.7 ± 1.0 ns observed in the case of the d(CpA*pC) adducts. Thus, quenching bases more distant than the flanking bases on the same strand influence the fluorescence yield and lifetimes of Py in the BPDE-*N*⁶-dA moieties. With the same (+)-*cis*-BPDE-*N*⁶-dA moieties in the 11-mer in a complex with the natural complementary strand, the mean fluorescence lifetime is also very short, i.e. 2.3 ± 0.2 ns (Table 1). These results clearly demonstrate that electron transfer fluorescence quenching reactions can occur with neighboring bases in these adducts, and that these effects depend on base composition and sequence, and possibly on the secondary structure of the DNA.

PHOTOCHEMICAL EFFECTS: DNA STRAND CLEAVAGE

The radical ion pairs generated by photoinduced electron transfer reactions in double-stranded BPDE-DNA duplexes can also decay by photochemical pathways giving rise to DNA damage. Two types of DNA damage are readily distinguishable, (1) direct or (frank) strand breaks and (2) chemically altered, or oxidized DNA nucleotides that can be converted to strand breaks upon hot alkali treatment (1 M piperidine at 90 °C for 30 min). These effects are demonstrated in the example shown in Fig. 4 using an oligonucleotide duplex containing a single, site-specifically placed modified guanine residue G* [where G* is (-)-*trans*-BPDE-*N*²-dG]. This oligonucleotide was labeled at the 5'-end with [³²P]ATP employing a standard T4 polynucleotide kinase 5'-terminus labeling system, and a duplex with its natural complementary strand was formed in 20 mM sodium phosphate buffer solution (pH 7.0). This solution was then irradiated with 355 nm light from a mercury-xenon lamp-monochromator system. After the irradiation, the solution was subjected to gel electrophoresis (20% denaturing polyacrylamide gel) in order to detect DNA fragments that may have resulted from the cleavage of the 5'-end-labeled, BPDE-modified oligonucleotide strand (Fig. 4). The shorter fragments migrate more rapidly and their lengths can be determined by comparing their mobilities with those observed with Maxam-Gilbert sequencing reactions obtained with the

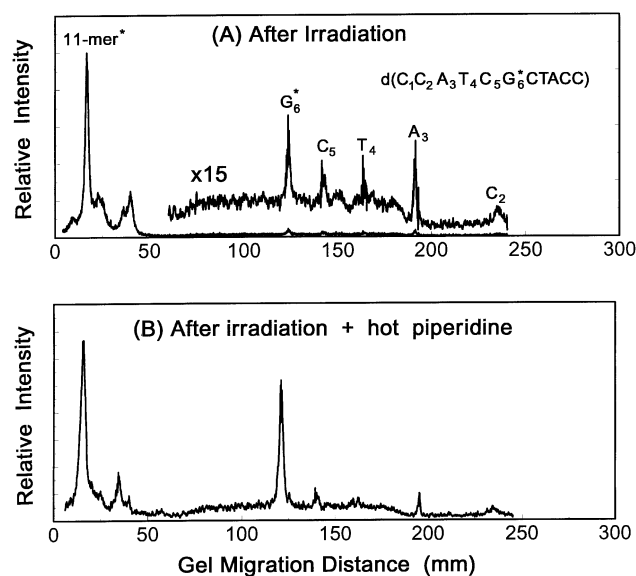


Figure 4. Phosphorimager analysis of autoradiographs of denaturing gel mobility patterns of fragments obtained after an 8 h illumination (355 nm light) of the Py residues in the 11-mer oligonucleotide duplex 5'-d(CCATCG*CTACC)●d(GGTAGCGATGG) (1 μ M) where G* = (-)-*trans*-BPDE-*N*²-dG. The modified strand was ³²P end-labeled, and the intact 11-mer oligonucleotide and the smaller fragment are identified in (A).

same oligonucleotide.⁸ In Fig. 4(A), the results are shown for samples that had been irradiated but not subjected to the hot piperidine treatment. The slowest moving and most prominent band on the left of the gel is due to the original, unmodified 11-mer; the sharp band at 39 mm on the horizontal axis is due to the 11-mer resulting from the photoinduced loss of the BPDE residue (this band and the neighboring still unidentified degradation bands with migration distances less than 50 mm comprise 57% of the initially present oligonucleotides). The bands labeled G*6 (0.6%), C5 (0.4%), T4 (0.5%), A3 (0.5%), and C2 (<0.4%) represent the different-sized fragments resulting from strand cleavage on the 5'-side of the G* residue at the indicated bases. It was shown in Ref. 88 that these small fragments co-migrate with Maxam-Gilbert cleavage fragments, and therefore have 3'-phosphate ends. The overall quantum yield of photodegradation is of the order of 10⁻⁶. The results shown in Fig. 4(A) indicate that reactive intermediates can migrate within the same strand from the site of generation at G6* to cause cleavage at the more distant sites C5, A3, C2 and C1 of the oligonucleotide (up to five base pairs from the site of excitation of the photosensitizer). This result is in agreement with our previous observations where we showed that strand cleavage occurs on both the 5'- and 3'-sides at distances up to 5-7 base pairs from the site of the photosensitizer-modified guanosyl residue.⁸ The fraction of oligonucleotides cleaved at G6* increases from 0.6% before piperidine treatment [Fig. 4(B)] to 9% after the hot

piperidine treatment. Overall, the fraction of intact oligonucleotide (100% before the irradiation) decreases to 41% after the irradiation and to 28% after the irradiation and the hot piperidine treatment.

Since the quantum yield of direct strand cleavage is of the order of 10^{-6} , this is an inefficient process, presumably because of the predominant non-radiative recombination of the intermediate radical ion pairs to the triplet and/or ground states of Py. The mobile reactive intermediates which give rise to cleavage at bases distant from the photoexcited Py residue may be holes, as suggested by Hall and Barton,² who observed hot alkali-labile sites at tandem GG bases distant from the sites of attachment of the metallointercalator photosensitizers. Similar kinds of oxidative damage at tandem GG bases have also been observed by Breslin and Schuster³ using substituted anthraquinone sensitizers as photonucleases. The elucidation of the chemical steps that occur subsequent to the excitation of the photosensitizer and the initial charge separation, and that ultimately lead to DNA strand cleavage at a distance, remains an interesting and challenging task. The ultimate resolution of this difficult problem will provide information, at new levels of detail, on the mechanisms by which photosensitizers cause DNA damage by Type I electron transfer mechanisms.¹⁰

Acknowledgments

This work was supported in part by the National Science Foundation (Grant CHE-9700429 to N.E.G.), and in part by an NIH fellowship to L. W. J. (Fellowship No. 1 F33 GM17908).

REFERENCES

1. T. Netzel. *J. Chem. Educ.* **74**, 646–651 (1997).
2. D. B. Hall and J. K. Barton. *J. Am. Chem. Soc.* **119**, 5045–5046 (1997).
3. D. T. Breslin and G. B. Schuster. *J. Am. Chem. Soc.* **118**, 2311–2319 (1996).
4. T. M. Netzel, K. Nafisi, J. Headrick and B. E. Eaton. *J. Phys. Chem.* 17948–17955 (1995).
5. L. P. A. Van Houte, R. van Grondelle, J. Retel, J. G. Westra, D. Zinger, J. C. Sutherland, S. K. Kim and N. E. Geacintov. *Photochem. Photobiol.* **49**, 387–394 (1989).
6. V. Ya. Shafirovich, P. P. Levin, V. A. Kuzmin, T. E. Thorgeirsson, D. S. Kliger and N. E. Geacintov. *J. Am. Chem. Soc.* **116**, 63–72 (1994).
7. V. Ya. Shafirovich, V. A. Kuzmin and N. E. Geacintov. *Chem. Phys. Lett.* **222**, 185–190 (1994).
8. B. Li, B. Mao, T.-M. Liu, J. Xu, A. Dourandin, S. Amin and N. E. Geacintov. *Chem. Res. Toxicol.* **8**, 396–402 (1995).
9. A. Marx, M. P. MacWilliams, T. A. Bickle, U. Schwitter and B. Giese. *J. Am. Chem. Soc.* **119**, 1131–1132 (1997).
10. I. E. Kochevar and D. A. Dunn. in *Bioorganic Photochemistry*, edited by H. Morrison, pp. 273–315 Wiley, New York (1990).
11. N. E. Geacintov, R. Zhao, V. A. Kuzmin, S. K. Kim and L. J. Pecora. *Photochem. Photobiol.* **58**, 185–194 (1993).
12. D. O'Connor, V. Y. Shafirovich and N. E. Geacintov. *J. Phys. Chem.* **98**, 9831–9838 (1994).
13. V. Ya. Shafirovich, S. H. Courtney, N. Ya and N. E. Geacintov. *J. Am. Chem. Soc.* **117**, 4920–4929 (1995).
14. V. Ibanez, N. E. Geacintov, A. G. Gagliano, S. Brandimarte and R. G. Harvey. *J. Am. Chem. Soc.* **102**, 5661–5666 (1980).
15. S. Steenken and S. V. Jovanovic. *J. Am. Chem. Soc.* **119**, 617–618 (1997).
16. C. A. M. Seidel, A. Schulz and M. H. M. Sauer. *J. Phys. Chem.* **100**, 5541–5553 (1996).
17. D. Rehm and A. Weller. *Isr. J. Chem.* **8**, 259–271 (1970).
18. B. E. Hingerty and S. Broyde. *Biopolymers* 2279–2299 (1985).